

## The Impact of pH Preparation on the Physical Nature and Metal Phase of Zeolite-Supported Metal Catalyst

Khoirina Dwi Nugrahaningtyas<sup>1\*</sup>, Anatta Wahyu Budiman<sup>2</sup>, Aji Indo Sabiila Gusti<sup>1</sup>, Eddy Herald<sup>1</sup>, and Yuniawan Hidayat<sup>1</sup>

<sup>1</sup>Department of Chemistry, Faculty of Mathematic and Natural Sciences, Sebelas Maret University, Surakarta, Jawa Tengah, Indonesia

<sup>2</sup>Department of Chemical Engineering, Faculty of Engineering, Sebelas Maret University, Surakarta, Jawa Tengah, Indonesia

Corresponding Author:

Khoirina Dwi Nugrahaningtyas  
khoirinadwi@staff.uns.ac.id

Received: February 2024

Accepted: July 2024

Published: September 2024

©Khoirina Dwi Nugrahaningtyas et al. This is an open-access article distributed under the terms of the Creative Commons Attribution License, which permits unrestricted use, distribution, and reproduction in any medium, provided the original author and source are credited.

### Abstract

The synthesis of CoMo/USY catalysts has been widely carried out. However, the bond strength between metal and USY is still a problem. Therefore, this research has synthesised the catalyst with the chelating agent ethylenediaminetetraacetate (EDTA). Apart from that, the effect of pH on the characteristics of the catalyst is also reviewed. This research aims to analyse the effect of preparation pH on catalyst characteristics. In the preparation process, the pH of the solution is set at values of 2, 7, and 8. Catalyst activation includes a calcination process and reduction. The catalyst characterisation uses XRD, GSA, and FTIR instruments to determine phase composition, specific surface area, and functional groups. The result showed that pH preparation significantly influenced the metal loading on the catalyst and reached a maximum at pH 8. The surface area is not directly related to the pH of the preparation but has the opposite property depending on the amount of metal added. Meanwhile, it was found that the CoO and MoO<sub>3</sub> phases were achieved on the catalyst by all pH preparations. On the other hand, the CoMo alloys are present on the catalyst at pH 7 and 8, while the Co and Mo elements are visible at pH 2. The difference in pH during the synthesis process impacts the shift in the absorption wave number of the OH vibration.

**Keywords:** CoMo/USY; Catalyst preparation; Chelating Agent; EDTA

### Introduction

Catalytic hydrotreatment is a purification reaction process in the presence of hydrogen and a catalyst to remove unwanted elements such as sulfur, nitrogen, and oxygen from oil to produce a green fuel. Catalysts for hydrotreatment reactions usually consist of active metals and supporting materials, where the active metals that have been widely developed are Co and Mo with Al<sub>2</sub>O<sub>3</sub> as

support [1]-[3]. The choice of support will affect active metal dispersion and activity. Therefore, to increase its catalytic activity, various materials such as carbon, TiO<sub>2</sub>, ZrO<sub>2</sub>, silica, alumina, modified silica, and zeolite have been tested as support materials for CoMo hydrogenation catalysts to find the most suitable support materials [4]-[10]. However, USY zeolite can be the most promising support material because its acidic site can increase catalytic activity and selectivity [10]-[12]. The

synergism effect of Co, Mo, and USY will produce a catalyst with a much higher hydrogenation activity.

The other way to improve catalytic activity is the use of chelating agents. Chelating agents are organic compounds that can bind to metal ions or multidentate ligands because they have more than one donor atom<sup>[5]</sup>. Ethylenediaminetetraacetate (EDTA) is one of the most popular chelating agents. In CoMo catalysts preparation, deprotonated EDTA binds to cobalt and produces complexes that are still together after the preparation and drying steps<sup>[13]</sup>. As complexes, cobalt ions are protected from direct interaction with support<sup>[5],[13]</sup> and delay activation<sup>[4],[5],[13]</sup>. Several kinds of researchers observed that EDTA additions could delay cobalt sulfidation, so minimizing the formation of the undesirable Co<sub>9</sub>S<sub>8</sub> phase and leading to the formation of promoted CoMoS phase<sup>[4]-[10],[13],[14]</sup>. Blanchard and coworkers studied that the chelating agent in CoMo catalysts limits the formation of Co<sub>3</sub>O<sub>4</sub>, followed by an increase of Co dispersion and catalytic activity<sup>[15]</sup>. Peña et al. (2014) studied that β-CoMoO<sub>4</sub> crystalline formation was avoided by EDTA addition in CoMo catalysts, leading to high Co dispersion<sup>[8]</sup>. Badoga and colleague also confirmed that EDTA addition has little effect on metal loading, decreases the metal particle size, and increases the metal dispersion<sup>[5]</sup>. Thus, EDTA addition as a chelating agent can improve the activity of catalysts in hydrogenation<sup>[4],[8],[16],[17]</sup>.

The characteristics of catalysts were influenced significantly by their preparation method. The most widely used metal-support catalyst preparation methods are impregnation, ion exchange, and precipitation. Previous research found that the catalyst prepared by the precipitation method had a high metal loading, surface area, and acid site values, so the activity was much higher than the catalyst prepared by impregnation<sup>[18]</sup>. The type of precipitant, metal salt, pH, aging time, and temperature influenced the characteristics of the catalyst for the catalyst synthesis reaction with the precipitation method. Meanwhile, pH in the preparation step is a critical parameter for

metal loading and particle size<sup>[19]</sup>, which consequently influences the activity of catalysts<sup>[1],[20],[21]</sup>.

The pH in the precipitation step can change the metals salt into hydroxides or another salt form, thus controlling metal loading on the support surface<sup>[22]</sup>. Song and coworkers studied that pH preparation influenced the metal loading and metal phase-type on catalysts<sup>[23]</sup>. In general, an increase in pH can increase the metal loading onto catalysts<sup>[19]</sup>. However, there are any limits for metal loading onto the support. Excessive metal loading causes metal agglomeration, resulting in the formation of large metal particles, and decreased metal dispersion. The excessive metal loading also decreased the average pore radius, pore volume, and surface area of the catalyst due to clogged pores<sup>[1],[20],[21]</sup>. In addition, metal loading also can influence the Bronsted acid sites on support material<sup>[20]</sup>, which can be indicated by infrared vibration shift of OH groups<sup>[24],[25]</sup>. Therefore, this study examined the effects of preparation pH on the physical characteristics and metal phases present in USY, drawing on prior research findings. Another innovative step in the metal deposition process on USY was the addition of EDTA, a chelating agent.

## Experimental

### Material

High silica zeolites of USY type (HSZ-341NHA) purchased from Tosoh Japan Corporation were calcined at 550 °C for 1 hour to obtain H-USY. Chemicals such as cobalt (II) nitrate, (NH<sub>4</sub>)<sub>6</sub>Mo<sub>7</sub>O<sub>24</sub>·4H<sub>2</sub>O, EDTA, and ammonia were bought from Merck with pro-analysis quality. Nitrogen and hydrogen gas were acquired from PT SAMATOR, Indonesia with more than 99% purity.

### Instruments

The instruments used in this research are X-ray Fluorosense (Brüker S2 Ranger), an X-ray diffractometer (XRD, Rigaku mini flex 600 benchtops, CuK radiation), Rietica software, Gas sorption analyzer (Quantachrome E 1600)

and Infrared spectroscopy (FTIR Shimadzu 8201 PC, KBr powder).

## Methods

### *Catalyst Preparation*

Co and Mo metals were loaded on H-USY by precipitation with the chelating agent EDTA. H-USY, EDTA (8% wt), and double distilled water were mixed in a two-neck flask at pH variations of 2, 7, and 8. The next step was the addition of the precursor metal salts of cobalt (2% wt) and molybdate (5.5% wt) simultaneously into the slurry while stirring slowly and heating at 60 °C for two hours. The precipitate was filtered and dried using a rotary evaporator at a pressure of 75 mBar and a temperature of 48°C. Dried samples were calcined and reduced under nitrogen (at 550 °C for three hours) and hydrogen (at 400 °C for two hours) gas streams.

### *Characterization*

The success of metal loading on the catalyst was detected using an X-ray Fluorescence (Bruker S2 Ranger) device. The impact of metal loading on the crystal structure of the catalyst was analyzed utilizing an X-ray diffractometer (XRD, Rigaku mini flex 600 benchtop, CuK radiation). Further analysis of the diffraction pattern of the catalyst using the Le Bail method with Rietica software to determine the type of impermeable metal phase. Meanwhile, the catalyst's texture analysis includes surface area, total pore volume, and average pore radius measured by a gas sorption analyzer (Quantachrome E 1600). Infrared spectroscopy (FTIR Shimadzu 8201 PC, KBr powder) was set up at a resolution of 2 cm<sup>-1</sup>, and the absorption pattern of its functional groups was observed at wavenumbers 400 - 4000 cm<sup>-1</sup>.

## Results and Discussion

### *Physical nature of CoMo/USY catalysts*

Based on Table 1, Co and Mo metals were successfully attached to support materials. The pH preparation significantly influenced the loading of cobalt and molybdenum. The

possibility of pH changes causes the metal ions to exchange into hydroxides, complexes, or other salts, leading to metal solubility modification [19],[22],[23]. So, metal particles can adhere to the pore surface of the USY support material, which in turn causes a transformation in the texture of the catalyst [20].

The pH in the preparation step influenced the form of Co and Mo, leading to solubility change [22]. The increases in pH have transformed Co ions into hydroxides and complexes [26]. Consequently, Co was straightforward to precipitate on the support surfaces. Meanwhile, molybdenum ions may transform into hydroxide at pH 3 – 6, and at pH 7, molybdenum beginnings to be dispersed in MoO<sub>4</sub><sup>2-</sup> ions form [22]. Although, in the presence of EDTA, molybdenum can form complexes with increased pH. Therefore, the Mo loading under pH 8 was decreased compared to pH 7 due to soluble MoO<sub>4</sub><sup>2-</sup> ions being washed out under the filtration step. Co and Mo were precipitated simultaneously on the catalysts under pH 7 due to forming hydroxides and complexes during the preparation process. Although, the Co loading at pH 7 was lower than pH 8 due to the competition with Mo to form complexes on the support surfaces. Nevertheless, Co and Mo were unchanged to hydroxides at pH 2, but they were found on the catalysts CoMo/USY-2. It was denoted that Co and Mo were locked in USY pores by another preparation method, such as impregnation under pH 2 [27].

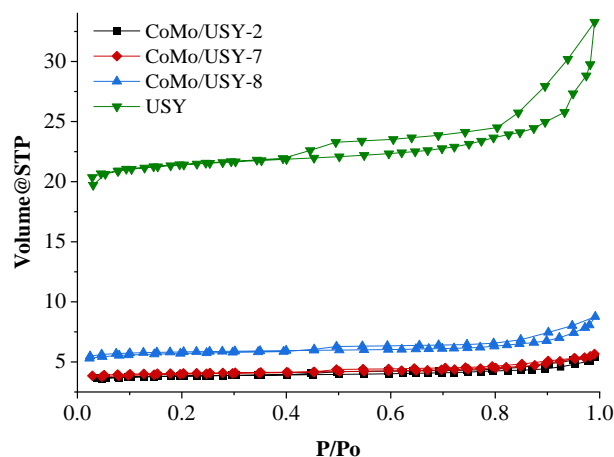
The specific surface area of CoMo/USY catalysts was higher than H-USY supports due to the presence of EDTA (Fig. 1). As a chelating agent, the EDTA is selective in extracting EFAL (extra framework aluminum) species from H-USY support [28]-[31], leading to the pore opening. The EFAL extraction can be detected by the Si/Al ratio raises, as shown in Table 1, due to the absence of alumina from EFAL species. However, pore opening was also evidenced by an increase in the specific surface area and pore volume and a decrease in pore size < 25.

**Table 1.** Physical nature of CoMo/USY catalysts

Sample	Elementals composition (%)					Specific surface area (m <sup>2</sup> /g)	Total pore volume (cm <sup>3</sup> /g) <sup>b</sup>	Average pore radius (Å)
	Co	Mo	Si	Al	Si/Al ratio			
H-USY	0.02	0.05	28.	8.03	3.49	405	0.31	15.37
CoMo/USY-2	2.08	1.41	35	6.97	5.04	506	0.35	14.28
CoMo/USY-7	1.05	3.20	25.	6.45	3.88	460	0.31	14.02
CoMo/USY-8	2.09	2.82	25	6.38	3.88	456	0.34	15.04

<sup>a</sup> CoMo/USY-x, where x is pH preparation

<sup>b</sup> Pores with a radius less than 1079.74 Å

**Figure 1.** Adsorption-desorption isotherm graph of N<sub>2</sub> gas from the catalyst.

CoMo/USY-2 was expressed as a catalyst with a higher Si/Al ratio, specific surface area, and pore volume. Therefore, this indicates that most of the EFAL species were extracted at pH 2. This study's results agree with the previous studies, which stated that at pH 2, EDTA had not yet formed a complex with Co and Mo [1],[20]-[26], so EDTA formed a complex with Al from EFAL. Meanwhile, the Al complexes formation reduced at pH 7 and 8 due to the competition with Co and Mo complexes.

The specific surface area of CoMo/USY catalysts was reduced with increases in metal loading. The metal particles attached to USY pores cause decreases in pore size and surface area. The influence of pH preparation on the pore

distribution has been further studied and described in Fig. 1. The pH preparation significantly influenced the pore with a radius of 15 – 80 Å. The pores with a size < 25 Å were reduced in the CoMo/USY-2 catalysts due to the EFAL extraction. The pores with a size < 25 in the CoMo/USY-7 catalyst were moderate compared to CoMo/USY-2 and USY, indicating that EFAL was reduced at pH 7. However, the pore volume was reduced, and several pores were formed around 20, 27, 34, 45, and 55 Å in the CoMo/USY-7 catalysts, thus indicating that the pore blocking was due to the metal loading on a support material. Based on pore distribution, the metals were observed to be well dispersed on the support material due to the chelating effect of EDTA ligands. Although,

it needs further confirmation with a scanning electron microscope (SEM) or others. However, the pores in the CoMo/USY-8 catalysts were most distributed around 50 Å, which might occur because of chelation rate was too fast, so the metals stacked and blocked the pores. However, this research cannot explain this phenomenon and needs further studies on chelation rates and complexes forming at various or higher pH levels.

### Metal phase type of CoMo/USY catalysts

The diffraction pattern of the H-USY supports and CoMo/USY catalysts are similar (Fig. 3). Thus, it indicates that metal loading did not significantly influence the crystal structure of H-USY supports. Co and Mo metals are not visible in the XRD spectra because these metals do not form crystals, or their intensity is under detection. Therefore, as in our previous publications, further analysis was carried out in this study to help determine the presence of metals in the catalyst<sup>[32]–[34]</sup>.

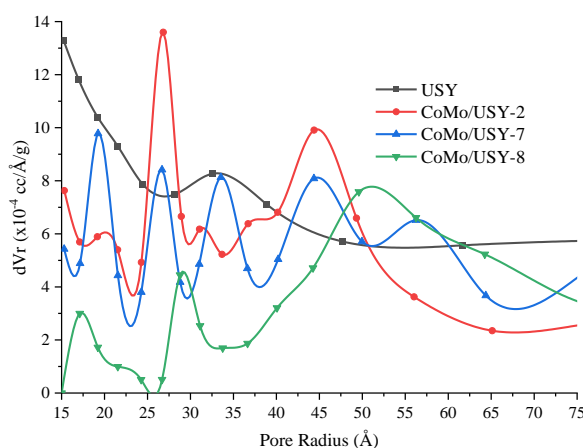


**Figure 2.** Pores distribution in the H-USY and CoMo/USY in the presence of EDTA (Pore radius 15 – 65 Å).

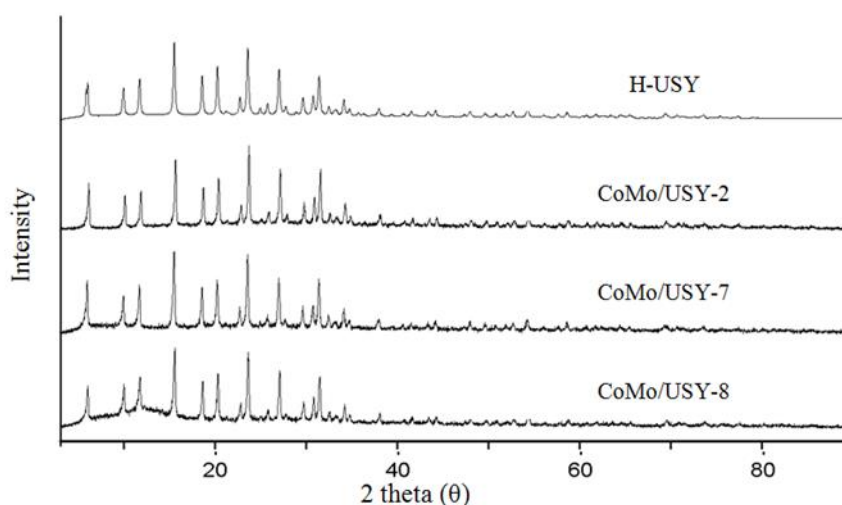


**Figure 3.** Diffraction pattern of H-USY and CoMo/USY catalysts under pH 2, 7, and 8 in the presence of EDTA.



The estimation of metal phase type under different pH preparation was conducted by Rietica application help using the Le Bail method with various relevance standards. The molar weight percentage of zeolite particles type with ICSD # 33599 and 26920 were obtained to be more than 97 % of the CoMo/USY catalysts. So, this confirmed the similarity between H-USY and CoMo/USY catalysts on XRD pattern. In addition, this method observed that some metal particles type could increase the molar weight of CoMo/USY catalysts, even only in small numbers.

Metal complexes, hydroxides, and salts were relatively easy to decompose by the calcination process, thus forming metal oxides such as CoO, MoO<sub>3</sub>, and CoMoO<sub>4</sub> (Table 2). However, the oxygen atom can be eliminated by further reduction, and a small number of Co, Mo, and CoMo metal phases were obtained on the catalysts. The Co and Mo particles disappeared in the increasing pH preparation, followed by the formation of CoMoO<sub>4</sub> and CoMo bimetal particles. The formation of CoMoO<sub>4</sub> and CoMo might indicate that Co and Mo metals were stacked together as complexes in the presence of EDTA, and they are close enough to be interacted and form bimetal in the catalyst's activation process. The EDTA as a chelating agent can form a complex with Co metals at pH 7 and 8, thus leading to a delay of Co oxidation in the calcination step [4]-[10],[13]-[15]. Thus, Co oxides can be limited [15], and Co with Mo metals can form a bimetal alloy. However, a metal that acts more as an active site in the hydrogenation reaction is the metal phase type

as an element [35]. For that reason, metal phase types, such as Co, Mo, or CoMo, have an essential role in the further hydrogenation reaction. The CoMo alloy may have different characteristics compared to Co and Mo element itself, thus make enjoyable to find out more about the activities of these CoMo/USY catalysts in the HDO reaction model.

### Functional Groups

The infrared spectrum of CoMo/USY catalysts, is similar to H-USY supports (Fig. 4). It is indicated that H-USY is kept as the primary component, and metal loading was not added or eliminated any functional group on the catalysts. The infrared spectrum shows the hydroxyl group, tetrahedral structure, and internal tetrahedral structure of USY.

The OH<sub>stretch</sub> shift of about 3400 cm<sup>-1</sup> occurs due to Co and Mo metals bound to the catalyst. The transmittances of the OH<sub>stretch</sub> on CoMo/USY catalysts were much higher than H-USY, except for CoMo/USY-2 catalysts. This OH<sub>stretch</sub> might represent Brönsted acid sites on the support material surface, which metals can reduce<sup>[24],[25]</sup>. The increases in OH<sub>stretch</sub> transmittance of CoMo/USY-7 and CoMo/USY-8 catalysts indicated that some -OH sites were lost because the metals could replace H<sup>+</sup> ions on the support surface. The OH<sub>stretch</sub> band shifted to a higher wave number in the presence of metals on the catalysts. The metals were attached to the support surface so to be close enough to the OH sites and influence the strength of -OH interactions [25].

**Table 2.** The phase type and composition of CoMo/USY catalysts

Standard Phase	ICSD number	Molar weight (%)		
		CoMo/USY-2	CoMo/USY-7	CoMo/USY-8
Zeolite-Y Na	33599	86.15	85.75	85.64
H-Faujasite	26920	11.02	10.93	10.90
CoO	245320	0.22	0.22	0.22
MoO <sub>3</sub>	644068	2.44	2.43	2.42
MoO <sub>3</sub>	158256	-	0.59	0.58
CoMoO <sub>4</sub>	281235	-	-	0.19
Co	622439	0.13	-	-
Mo	173127	0.05	0.04	-

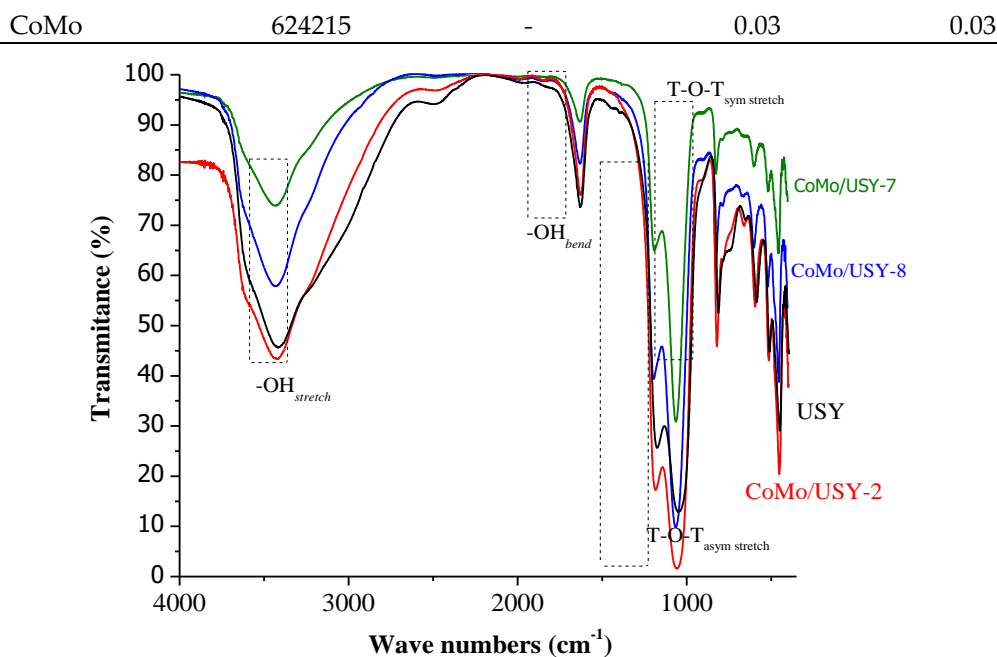


**Figure 4.** Infrared spectroscopy of H-USY and CoMo/USY catalysts under pH 2, 7, and 8 in the presence of EDTA.

**Table 3.** Infrared spectroscopy of H-USY supports and CoMo/USY catalysts.

Functional group	Vibration wave number (cm <sup>-1</sup> )			
	H-USY	CoMo/USY-2	CoMo/USY-7	CoMo/USY-8
O-H stretch	3397.79	3439.23	3425.72	3425.72
O-H bend	1634.79	1623.17	1627.99	1631.85
T-O-T asym stretch	1178.56	1189.17	1191.09	1195.92
	1051.25	1060.89	1063.79	1064.75
T-O-T sym stretch	816.89	825.57	826.53	827.5
	742.63	788.92	786.03	785.06
T-O internal asym stretch	454.26	457.15	456.18	456.18
T-O internal sym stretch	657.75	664.51	670.29	676.08

The shifted adsorption wave number of the T-O-T sym stretch and T-O-T asym stretch toward a large wave number is in line with the increased amount of implanted metal. That indicates that the metal imposition presses the USY framework, making it difficult to vibrate the T-O-T bond (T = Si or Al). The shift in the absorption wave number due to the addition of metal and the difference in pH are briefly described in Table 3.

## Conclusions

CoMo/USY catalysts were successfully prepared by precipitation under pH 2, 7, and 8 in the presence of EDTA. The metal loading on the catalysts was influenced by pH preparation, and CoMo/USY-8 was observed as the catalysts with higher metal loading. The Co and Mo particle types were only obtained on CoMo/USY-2 catalysts and disappeared with

increasing pH preparation, followed by the formation of CoMoO<sub>4</sub> and CoMo. The pH preparation also influenced the catalysts' surface area and –OH functional group. Co and Mo metals were attached to support the surface and reduce the pores volume and surface area of catalysts. The metals were also close enough to the –OH groups on the support surface, influencing the –OH interaction. In this case –OH interactions became much stronger. The decreased number of –OH groups on CoMo/USY-7 and CoMo/USY-8 catalysts is due to the ion exchange between H<sup>+</sup> and metal ions. Based on metal loading, CoMo/USY-8 catalysts were the best but based on surface area and the number of –OH groups, CoMo/USY-2 can be considered the best catalysts for the hydrogenation reaction.

#### Acknowledgments

The authors would like to thank the Indonesian Ministry of Education, Culture, Research and Technology for funding this research through Hibah Fundamental Regular with contract number: 1280.1/UN27.22/PT.01.03/2023.

#### References

1. Nikulshin, P. A., Mozhaev, A. V., Pimerzin, A. A., Konovalov, V. V. & Pimerzin, A. A., CoMo/Al<sub>2</sub>O<sub>3</sub> catalysts prepared on the basis of Co 2Mo 10-heteropolyacid and cobalt citrate: Effect of Co/Mo ratio. in *Fuel*, **100**: 24–33 Elsevier Ltd, (2012).
2. Herrera, J. E., Balzano, L., Borgna, A., Alvarez, W. E. & Resasco, D. E., Relationship between the Structure/Composition of Co–Mo Catalysts and Their Ability to Produce Single-Walled Carbon Nanotubes by CO Disproportionation. *J. Catal.*, **204**(1): 129–145 (2001).
3. Rochet, A., Baubet, B., Moizan, V., Pichon, C. & Briois, V., Co-K and Mo-K edges Quick-XAS study of the sulphidation properties of Mo/Al<sub>2</sub>O<sub>3</sub> and CoMo/Al<sub>2</sub>O<sub>3</sub> catalysts. *Comptes Rendus Chim.*, **19**(10): 1337–1351 (2016).
4. Badoga, S., Dalai, A. K., Adjaye, J. & Hu, Y., Insights into individual and combined effects of phosphorus and EDTA on performance of NiMo/MesoAl<sub>2</sub>O<sub>3</sub> catalyst for hydrotreating of heavy gas oil. *Fuel Process. Technol.*, **159**: 232–246 (2017).
5. Badoga, S., Mouli, K. C., Soni, K. K., Dalai, A. K. & Adjaye, J., Beneficial influence of EDTA on the structure and catalytic properties of sulfided NiMo/SBA-15 catalysts for hydrotreating of light gas oil. *Appl. Catal. B Environ.*, **125**: 67–84 (2012).
6. Badoga, S., Sharma, R. V., Dalai, A. K. & Adjaye, J., Hydrotreating of heavy gas oil on mesoporous zirconia supported NiMo catalyst with EDTA. *Fuel*, **128**: 30–38 (2014).
7. Al-Dalama, K. & Stanislaus, A., Temperature programmed reduction of SiO<sub>2</sub>–Al<sub>2</sub>O<sub>3</sub> supported Ni, Mo and NiMo catalysts prepared with EDTA. *Thermochim. Acta*, **520**(1–2): 67–74 (2011).
8. Peña, L., Valencia, D. & Klimova, T., CoMo/SBA-15 catalysts prepared with EDTA and citric acid and their performance in hydrodesulfurization of dibenzothiophene. *Appl. Catal. B Environ.*, **147**: 879–887 (2014).
9. Ramírez, J., Romualdo-Escobar, D., Castillo-Villalón, P. & Gutiérrez-Alejandre, A., Improved NiMoSA catalysts: Analysis of EDTA post-treatment in the HDS of 4,6-DMDBT. *Catal. Today*, **349**: 168–177 (2020).
10. He, Z. & Wang, X., Hydrodeoxygenation of model compounds and catalytic systems for pyrolysis bio-oils upgrading. *Catal. Sustain. Energy, Versita*, **1**(2013): 28–52 (2012).
11. Maesen, T. L. M., Calero, S., Schenk, M. & Smit, B., Alkane hydrocracking: shape selectivity or kinetics? *J. Catal.*, **221**(1): 241–251 (2004).
12. Ding, L., Zheng, Y., Zhang, Z., Ring, Z. & Chen, J., HDS, HDN, HDA, and hydrocracking of model compounds over



- Mo-Ni catalysts with various acidities. *Appl. Catal. A Gen.*, **319**: 25–37 (2007).
13. van Haandel, L., Bremmer, G. M., Hensen, E. J. M. & Weber, T., The effect of organic additives and phosphoric acid on sulfidation and activity of (Co)Mo/Al<sub>2</sub>O<sub>3</sub> hydrodesulfurization catalysts. *J. Catal.*, **351**: 95–106 (2017).
  14. Sundaramurthy, V., Dalai, A. K. & Adjaye, J., Effect of EDTA on hydrotreating activity of CoMo/ $\gamma$ -Al<sub>2</sub>O<sub>3</sub> catalyst. *Catal. Lett.* 2005 **102**(3): 299–306 (2005).
  15. Blanchard, P., Mauchausse, C., Payen, E., Grimblot, J., Poulet, O., Boisdron, N. & Loutaty, R., Preparation and characterization of CoMo/Al<sub>2</sub>O<sub>3</sub> HDS catalysts: Effects of a complexing agent. *Stud. Surf. Sci. Catal.*, **91**(C): 1037–1049 (1995).
  16. Rana, M. S., Ramírez, J., Gutiérrez-Alejandre, A., Ancheyta, J., Cedeño, L. & Maity, S. K., Support effects in CoMo hydrodesulfurization catalysts prepared with EDTA as a chelating agent. *J. Catal.*, **246**(1): 100–108 (2007).
  17. Lérias, M. A., Le Guludec, E., Mariey, L., van Gestel, J., Travert, A., Oliviero, L. & Maugé, F., Effect of EDTA addition on the structure and activity of the active phase of cobalt–molybdenum sulfide hydrotreatment catalysts. *Catal. Today*, **150**(3–4): 179–185 (2010).
  18. Ahmad, R., Schrempp, D., Behrens, S., Sauer, J., Döring, M. & Arnold, U., Zeolite-based bifunctional catalysts for the single step synthesis of dimethyl ether from CO-rich synthesis gas. *Fuel Process. Technol.*, **121**: 38–46 (2014).
  19. Koo, K. Y., Park, M. G., Jung, U. H., Kim, S. H. & Yoon, W. L., Diesel pre-reforming over highly dispersed nano-sized Ni catalysts supported on MgO–Al<sub>2</sub>O<sub>3</sub> mixed oxides. *Int. J. Hydrogen Energy*, **39**(21): 10941–10950 (2014).
  20. Barton, R. R., Carrier, M., Segura, C., Fierro, J. L. G., Escalona, N. & Peretti, S. W., Ni/HZSM-5 catalyst preparation by deposition-precipitation. Part 1. Effect of nickel loading and preparation conditions on catalyst properties. *Appl. Catal. A Gen.*, **540**(March): 7–20 (2017).
  21. Bose, S. & Das, C., Preparation, characterization, and activity of  $\gamma$ -alumina-supported molybdenum/cobalt catalyst for the removal of elemental sulfur. *Appl. Catal. A Gen.*, **512**: 15–26 (2016).
  22. Van Dillen, A. J., Terörde, R. J. A. M., Lensveld, D. J., Geus, J. W. & De Jong, K. P., Synthesis of supported catalysts by impregnation and drying using aqueous chelated metal complexes. *J. Catal.*, **216**(1–2): 257–264 (2003).
  23. Song, S., Sheng, Z., Liu, Y., Wang, H. & Wu, Z., Influences of pH value in deposition-precipitation synthesis process on Pt-doped TiO<sub>2</sub> catalysts for photocatalytic oxidation of NO. *J. Environ. Sci.*, **24**(8): 1519–1524 (2012).
  24. Mhamdi, M., Khaddar-Zine, S., Ghorbel, A., Marceau, E., Che, M., Ben Taarit, Y. & Villain, F., Characterization of Co-ZSM-5 catalysts prepared by solid-state exchange: influence of Co/Al ratio on cobalt speciation and catalytic properties. *Stud. Surf. Sci. Catal.*, **158**: 749–756 (2005).
  25. Mendes, P. S. F., Lapisardi, G., Bouchy, C., Rivallan, M., Silva, J. M. & Ribeiro, M. F., Hydrogenating activity of Pt/zeolite catalysts focusing acid support and metal dispersion influence. *Appl. Catal. A Gen.*, **504**: 17–28 (2015).
  26. Huang, J. H., Kargl-Simard, C., Oliazadeh, M. & Alfantazi, A. M., pH-Controlled precipitation of cobalt and molybdenum from industrial waste effluents of a cobalt electrodeposition process. *Hydrometallurgy*, **75**(1–4): 77–90 (2004).
  27. Alsobaai, A. M., Hameed, B. H. & Zakaria, R., Hydrocracking of Gas Oil using USY-Zeolite-Based Catalyst. 243–254 (2006).
  28. Agudelo, J. L., Mezari, B., Hensen, E. J. M., Giraldo, S. A. & Hoyos, L. J., On the effect of EDTA treatment on the acidic properties

- of USY zeolite and its performance in vacuum gas oil hydrocracking. *Appl. Catal. A Gen.*, **488**: 219–230 (2014).
29. Gola, A., Rebours, B., Milazzo, E., Lynch, J., Benazzi, E., Lacombe, S., Delevoye, L., *et al.*, Effect of leaching agent in the dealumination of stabilized Y zeolites. *Microporous Mesoporous Mater.*, **40(1–3)**: 73–83 (2000).
30. Qiao, K., Li, X., He, L., Liu, X., Yan, Z., Xing, W., Qin, L., *et al.*, An efficient modification of ultra-stable Y zeolites using citric acid and ammonium fluosilicate. *Appl. Petrochemical Res.* 2014 **44**, **4(4)**: 373–378 (2014).
31. Xu, B., Bordiga, S., Prins, R. & van Bokhoven, J. A., Effect of framework Si/Al ratio and extra-framework aluminum on the catalytic activity of Y zeolite. *Appl. Catal. A Gen.*, **333(2)**: 245–253 (2007).
32. Nugrahaningtyas, K. D., Putri, M. M. & Saraswati, T. E., Metal phase and electron density of transition metal/HZSM-5. in *AIP Conference Proceedings*, **2237(June)**: 020003 (2020).
33. Nugrahaningtyas, K. D., Suharbiansah, R. S. R., Lestari, W. W. & Rahmawati, F., Metal Phase, Electron Density, Textural Properties, and Catalytic Activity of CoMo Based Catalyst Applied in Hydrodeoxygenation of Oleic Acid. *Evergreen*, **9(2)**: 283–291 (2022).
34. Sabailagusti, A. I., Nugrahaningtyas, K. D. & Hidayat, Y., Synthesis and Metal Phases Characterization of Mordenite Supported Copper Catalysts. *J. Phys. Conf. Ser.*, **1912(1)**: 012032 (2021).
35. Augustine, R. L. & Tanielyan, S. K., Enantioselective heterogeneous catalysis. 2. Examination of the formation of the individual (R) and (S) lactates in the cinchonidine modified platinum hydrogenation of pyruvate. *J. Mol. Catal. A Chem.*, **112(1)**: 93–104 (1996).